



Experimental investigation on reservoir damage caused by clay minerals after water injection in low permeability sandstone reservoirs

Yazhou Zhou^{1,2} · Wenbin Yang^{1,2} · Daiyin Yin^{1,2}

Received: 8 July 2021 / Accepted: 23 October 2021 / Published online: 31 October 2021
© The Author(s) 2021

Abstract

Water injection is an effective method for developing low permeability sandstone reservoirs. In the process of water flooding, reservoir damage can occur due to clay mineral content changes and it will significantly affect oil production. There are few investigations on the changes in clay mineral content and the degree of reservoir damage after injecting the water into low permeability sandstone reservoirs with different permeabilities and lithologies. In this study, low permeability natural cores from different lithological strata were collected from 4 wells in the Daqing sandstone reservoir, and clay mineral components and contents were measured through X-ray diffraction. Changes in the clay mineral content were determined after water injection. The reservoir damage mechanism by clay mineral migration was determined by analyzing scanning electron microscopy (SEM) images after water injection. Meanwhile, the porosity and permeability of the cores were tested after water injection, and the degree of reservoir damage in different lithological strata was determined. The clay mineral content ranges from 6.78 to 14.14% in low permeability sandstone cores and declines by 49.73% after water flooding. Illite, chlorite and illite/smectite mostly decrease, and kaolinite decreases the least. Due to the large particle size of kaolinite, kaolinite migration will block the pore-throats and cause formation damage after water flooding. In argillaceous siltstone and siltstone, kaolinite particles blocking pore-throats are very serious, and the permeability decreases greatly by 21.87–36.89% after water injection. With increasing permeability, the permeability decreases greatly after water injection. The findings of this study can help to better understand the mechanisms of formation damage after injecting water into low permeability sandstone reservoirs.

Keywords Low permeability sandstone reservoir · Reservoir damage · Clay minerals · Kaolinite · Water Flooding

Introduction

In petroleum reservoirs, the maximum oil recovery of natural drives is only 20–60% (Zhou et al. 2019), and it is much lower in low permeability reservoirs (Zheng et al. 2009). There are enormous low permeability resources around the world. In China, low permeability reservoir resources account for more than 40% of the total resources. Most low permeability reservoirs are developed by injecting water (Wang et al. 2019c). In low permeability reservoirs, the

pore-throat radius is much smaller than that of high permeability reservoirs (Zhou et al. 2018; Zhang et al. 2017). Moreover, the start-up pressure gradient is large in low permeability reservoirs (Li et al. 2016), and the recovery efficiency is low in water injection development (Demirel 2005; Wang et al. 2019b; Peng et al. 2006). In addition, formation damage occurs more easily in low permeability sandstone reservoirs, and the formation damage includes water sensitivity damage, acid sensitivity damage, alkali sensitivity damage and velocity sensitivity damage. The water-sensitive minerals are chlorite-montmorillonite, illite, chlorite, and white mica, which can expand, disperse and migrate in the pores and pore-throats (Wang et al. 2019a). The acid-sensitive minerals are chlorite, ferrodolomite, hematite, glauconite, pyrite, white mica, limestone, dolomite, anorthite and clay minerals, which can react with HCl and HF, generating chemical precipitation (Baker et al. 1993). Alkali-sensitive minerals include potash feldspar, soda feldspar, plagioclase

✉ Yazhou Zhou
zhouyazhou720@163.com

¹ Department of Petroleum Engineering, Northeast Petroleum University, Daqing, China

² Key Laboratory of Enhanced Oil Recovery, Ministry of Education, Northeast Petroleum University, Daqing, China

and clay minerals, which can react with alkalis, generating silicate precipitation (Ma et al. 2016). The velocity-sensitive minerals are kaolinite, illite and white mica, which can disperse and migrate in pores and pore-throats, blocking the pore-throats (Kamal et al. 2019). Clay minerals are an important component of low permeability sandstone reservoirs. Clay mineral components and contents will change due to the development of long-term water injection (Jiang et al. 2012; Strand et al. 2007), and they influence the microscopic porous structures and microscopic seepage characteristics in low permeability reservoirs. Some clay minerals are damaged during injection water development (Cosenza et al. 2014; Yue et al. 2011; Jain et al. 2016). The destroyed clay mineral particles are dispersed and are able to migrate with the injected water. Some clay mineral particles are produced in the water and crude oils in the oil wells, and others accumulate in micropores or throats (Grude et al. 2015; Stück et al. 2013; An et al. 2016; Meng et al. 2015; Sadhukhan et al. 2007). Because the pores and pore-throats are small in size, clay mineral migration will influence the porous structure and seepage characteristics (Reuvers and Golombok 2009; Law et al. 2015; Wang et al. 2019d). Currently, there are many studies on formation damage after water flooding and how to reduce formation damage in low permeability sandstone reservoirs (Olayiwola and Dejam 2020). However, few studies have examined the change in clay mineral content for reservoirs with different permeabilities. Few studies have provided a quantitative analysis on the degree of reservoir damage after water flooding for different lithologic reservoirs, and there is limited knowledge about the damage caused by clay minerals from water injection in low permeability sandstone reservoirs. To investigate the formation damage after long-term water flooding in a low permeability sandstone reservoir, first, different lithological cores were collected from 4 wells in a low permeability sandstone reservoir of the Daqing Oilfield. X-ray diffraction and SEM were adopted to determine the changes in

clay mineral content after water flooding. Then, the reservoir damage mechanisms induced by the clay minerals were analyzed. Finally, the degree of damage in the different lithological strata is discussed, as shown in Fig. 1. It can provide insight into water injection development in low permeability sandstone reservoirs.

Materials and methods

Materials

The low permeability sandstone reservoirs of Daqing Oilfield were investigated and natural cores from 4 wells were used in this study. These natural cores represent argillaceous siltstone, siltstone and fine sandstone, respectively. Data from the cores are listed in Table 1. The cores were cylindrical and were $\Phi 2.5 \times 10$ cm in size. To prevent hydration expansion of clay minerals, formation water flooding displacement was simulated, and the salinity of the simulated formation water was 8200 mg/L.

Experimental instruments

An HW-4A double thermostat, an ISCO pump, a Welch1402 vacuum pump, X-ray diffraction, scanning electron microscopy, and a gas permeability tester were used in the study.

Experimental methods

X-ray diffraction test of clay mineral contents

Experimental steps of the X-ray diffraction test include:

- (1) Natural cores were dried for 24 h at 60 °C, and some samples were collected for X-ray diffraction analysis.

Fig. 1 The general overview of the investigation

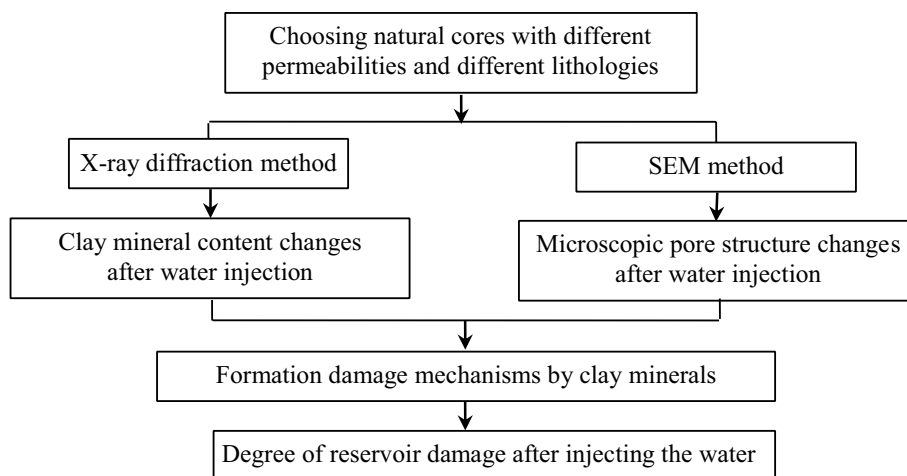


Table 1 The lithology, well, depth, porosity, and permeability of the natural cores

Core Number	Lithology	Cored well	Depth (m)	Porosity (%)	Permeability ($10^{-3}\mu\text{m}^2$)
#3	Argillaceous siltstone	M7-1-J33	964.0–964.8	20.7	4.8
#14	Argillaceous siltstone	M1-D3-J323	985.3–986.5	20.1	6.9
#19	Argillaceous siltstone	M1-D3-J323	943.0–944.0	21.2	10.7
#20	Siltstone	M7-1-J33	1006.8–1007.6	22.1	14.6
#23	Siltstone	M7-1-J33	1005.6–1009.1	21.2	18.7
#24	Siltstone	M1-D3-J323	1041.6–1045.0	23.4	24.5
#28	Fine sandstone	M1-D3-J323	1047.4–1049.9	22.7	36.8
#30	Fine sandstone	M7-1-J33	991.5–994.7	22.8	42.1
#31	Fine sandstone	M7-1-J33	998.8–1004.0	24.1	54.1

These samples were crushed and ground to fine particles with particle sizes lower than 40 μm .

- (2) Particles smaller than 10 μm were extracted from the samples through free settling. After an equivalent amount of corundum was added, subsamples were collected to test the contents of different minerals through an X-ray diffraction meter.
- (3) The remaining part of the samples were transferred into a suspension liquid. Samples with particle sizes smaller than 2 μm were extracted, and the suspension was centrifuged to settle the clay minerals.
- (4) Distilled water was added to the centrifuged clay minerals, and the mixture was mixed evenly. The mixture was then coated onto a glass slide and air-dried, and natural orienting slices (N slices) were made. Diffraction spectra of the N slices were tested.
- (5) N slices were saturated in an ethanediol stream for 8 h, forming ethanediol saturated slices (EG slices). Diffraction spectra of the EG slices were tested.
- (6) Ethanediol-saturated slices were placed at a constant temperature of 500 °C for 3 h and then cooled to room temperature naturally. High-temperature slices were created and the corresponding diffraction patterns were tested.
- (7) The relative contents of clay minerals were analyzed by an X-ray diffraction analysis instrument.

Testing the porosity and permeability before and after water flooding

The permeability and porosity of the natural cores were determined after being saturated in simulated formation water at 45 °C. Then, water was injected into the natural cores at a rate of 0.15 mL/min. The accumulative injected water was 100 PV (pore volume). The permeability of the cores was tested, and the porosity was measured after cleaning.

Clay mineral contents after water injection

During water development in low permeability sandstone reservoirs, clay mineral changes are important factors that cause reservoir damage (Sameni et al. 2015). Before and after injecting the water, the clay mineral contents of the natural cores were tested by X-ray diffraction, and the results are shown in Table 2. Changes in clay minerals in the different lithological cores were analyzed, and the results are shown in Table 3 and Figs. 2, 3 and 4.

According to the experimental results, the low permeability sandstone reservoir in the Daqing Oilfield contains 4 clay minerals: illite, kaolinites, chlorite and illite/smectite formations, and the illite and chlorite contents are the highest. When the permeability ranges from 4.8×10^{-3} to $54.1 \times 10^{-3} \mu\text{m}^2$, the total clay mineral content ranges from 6.78 to 14.14%. The clay mineral content decreases with increasing permeability. After injecting the water, the clay mineral contents decreased by 49.73% on average, which indicates partial clay mineral migration out of cores with water injection. The contents of illite, illite/smectite formation and chlorite decrease, mostly due to their small grain size. The contents of illite, illite/smectite formation and chlorite decrease by 57.48, 55.50 and 48.22%, respectively, after injecting the water. As the grain size of kaolinite is larger than that of the other clay minerals, most kaolinite particles cannot pass through the pore-throat channels with the injected water, and most kaolinites cannot flow out with fluid. After injecting the water, the content of kaolinite decreased by 32.56% on average. For the different lithological cores, the permeability and porosity increase from the argillaceous siltstone to the fine sandstone, and the kaolinite content is reduced to a greater extent after injecting water. The porosity and permeability of the argillaceous siltstone are the lowest, and the radii of the rock pores and pore-throat channels are the smallest. The content of kaolinite decreases by 17.80%

Table 2 The variation in clay content after water injection

Core number	Lithology	Illite content (%)		Kaolinite content (%)		Chlorite content (%)		Illite/smectite content (%)		Total clay content (%)	
		Original	After water injection	Original	After water injection	Original	After water injection	Original	After water injection	Original	After water injection
#3	Argillaceous siltstone	7.46	3.38	1.31	1.10	3.85	1.91	1.53	0.48	14.14	6.87
#14	Argillaceous siltstone	2.84	1.09	2.62	2.29	2.69	1.39	1.06	0.30	9.19	5.08
#19	Argillaceous siltstone	6.52	2.81	1.81	1.32	3.62	1.82	1.43	0.32	13.37	6.25
#20	Siltstone	3.48	1.12	1.35	0.81	3.45	0.93	0.25	0.18	8.53	3.04
#23	Siltstone	2.64	0.68	1.50	1.01	2.91	1.91	1.27	0.57	8.32	4.17
#24	Siltstone	2.71	1.13	1.42	0.92	2.51	1.41	0.86	0.70	7.50	4.16
#28	Fine sandstone	2.51	1.15	1.67	0.89	2.53	1.53	0.66	0.30	7.37	3.87
#30	Fine sandstone	2.43	1.42	1.75	0.96	2.37	1.32	0.36	0.31	6.91	4.01
#31	Fine sandstone	2.38	1.24	1.68	0.89	2.41	1.42	0.31	0.28	6.78	3.83

after injecting the water, indicating that most kaolinite accumulates in the pores and pore-throats. The radii of the pores and pore-throats of the siltstone are higher than those of the argillaceous siltstone. The content of kaolinite decreases by 35.92% after injecting the water. Since the radii of the pores and pore-throats in the fine sandstones are higher than those of in the argillaceous siltstone and siltstone, the contents of kaolinite decreased significantly by 46.47% after injecting the water, indicating that most kaolinites migrate out of the cores with the injected water.

Formation damage mechanisms by clay minerals

The distribution and the forms of clay minerals in the pores and pore-throat channels were observed by SEM after injecting the water. The microscopic damage mechanism of clay minerals was analyzed after injecting water into low permeability sandstone cores. The microscopic formation damage mechanism of clay minerals includes illite assembly on the core surface, kaolinite blockades in the pores and pore-throat channels and chlorite blockades in the pores and pore-throat channels.

(1) Illite assembling on the surface of the cores.

Illite is the most common clay mineral cement in sandstone. It has one of the most complex morphologic changes in clay minerals. According to SEM observations, most illite is flaky and adheres to particle surfaces within the cores before water injection. The particle size of illite is uneven, ranging from 0.15 to 2.5 μm , and has irregular edges, as shown in Fig. 5. After long-term injection of water, approximately 50% of the illite migrates out of the cores with the injected water, and a small amount assembles on the pore-throat surfaces. This causes fluid flow in the channel to decrease.

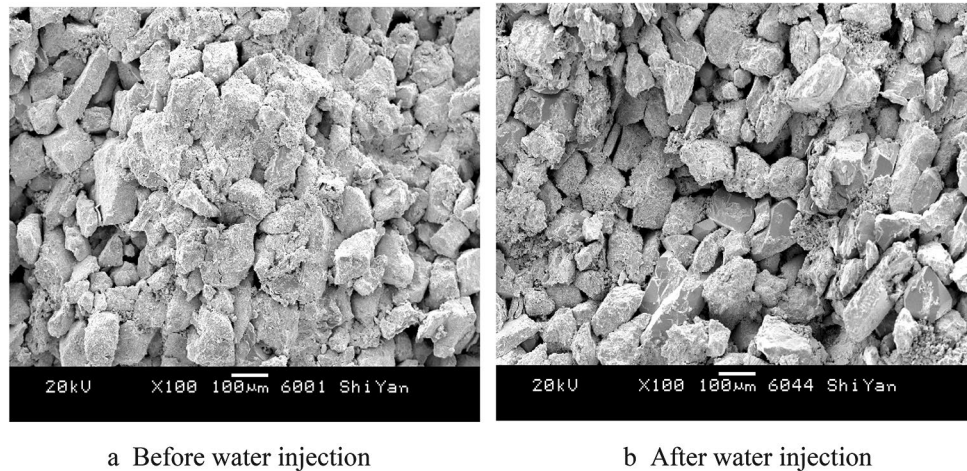
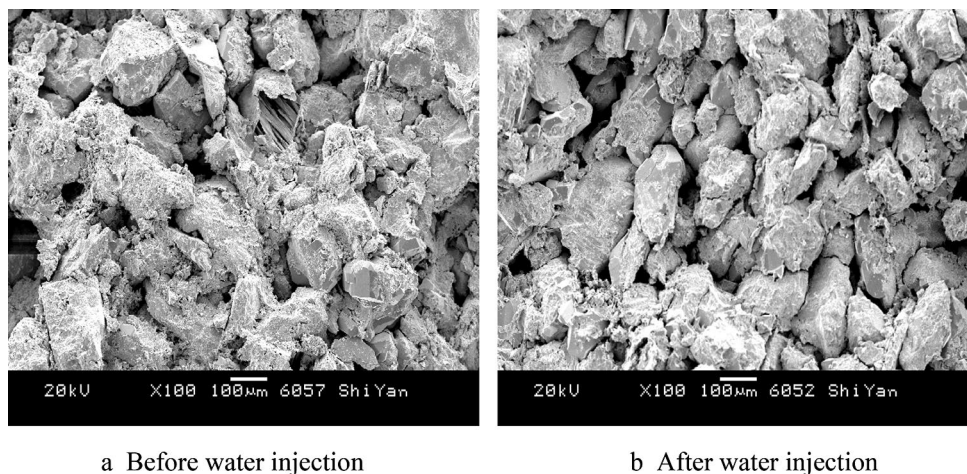
(2) Kaolinite blocks pores and pore-throats.

Kaolinite often fills the pores of sandstones and aggregates in book and worm-like structures. The grain size of kaolinite generally ranges from 1.0 to 6.0 μm . After long-term injection of water, some kaolinite falls off from the clastic particles and is broken into pieces, where it will then flow with the fluid into the pores and pore-throat channels. This easily causes pores and pore-throat blockages, as shown in Fig. 6. Due to the small radius of pore-throat channels in argillaceous siltstone and siltstone, blockages by kaolinite particles are very serious after water injection. In contrast, kaolinite blockages of the pore-throat channels is less in fine sandstone due to the large radii of the channels.

(3) Chlorite blocks pores and pore-throats.

Table 3 The variation in clay content for different lithological cores after water injection

Lithology	Illite content (%)		Kaolinite content (%)		Chlorite content (%)		Illite/smectite content (%)		Total clay content (%)	
	Original	After water injection	Original	After water injection	Original	After water injection	Original	After water injection	Original	After water injection
Argillaceous siltstone	5.61	2.43	1.91	1.57	3.39	1.71	1.34	0.37	12.23	6.07
Siltstone	2.94	0.98	1.42	0.91	2.96	1.42	0.79	0.48	8.12	3.79
Fine sandstone	2.44	1.27	1.70	0.91	2.44	1.42	0.44	0.30	7.02	3.90

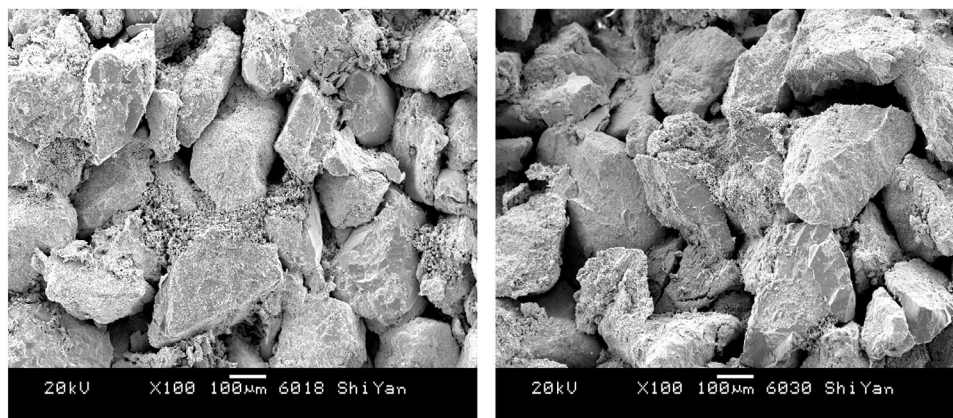
Fig. 2 Changes in the argillaceous siltstone after water injection**Fig. 3** Changes in the content of siltstone after water injection

According to SEM observations, chlorite is willow-shaped and adheres to particle surfaces or fills pores as aggregates. The grain size of chlorite is generally smaller than 0.8 μm , as shown in Fig. 7. After injecting the water, nearly 50% of the chlorite is washed out

by the water, and a small amount of the particles are blocked in the pores and throats, as shown in Fig. 8.

There is a low content of illite/smectite formation in the rocks, and most illite/smectite formations adhere to clastic

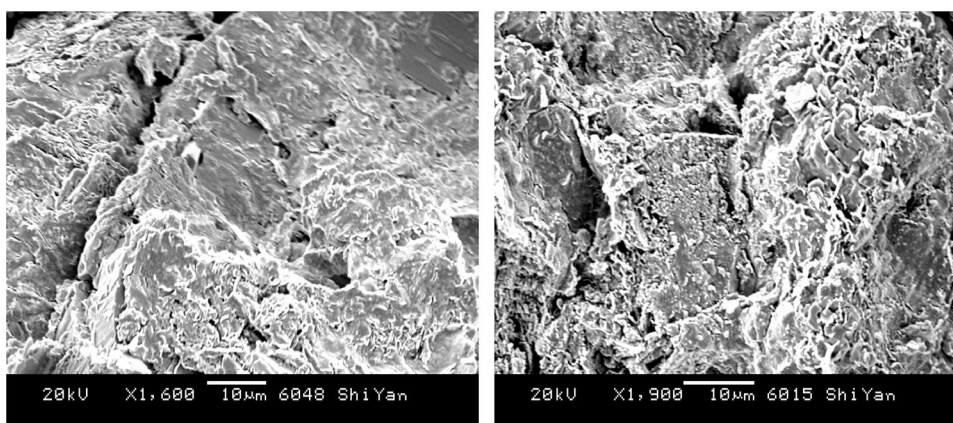
Fig. 4 Changes in the fine sandstone content after water injection



a Before water injection

b After water injection

Fig. 5 Illite assembled on particle surfaces



particle surfaces as thin films. The illite/smectite formation content changes slightly after injecting the water, and it is not a major cause of blockages in the reservoir. Therefore, kaolinite blockages in the pores and pore-throat channels are the principle cause of formation damage by clay minerals after water injection in low permeability sandstone reservoirs. Kaolinite blockages will be more serious in argillaceous siltstones and siltstone formations than in fine sandstones.

Degree of reservoir damages after water injection

Porosity and permeability were tested after injecting the water, and the results are shown in Table 4. A comparison of permeability changes in different lithological cores is shown in Fig. 9.

The porosity of the cores changes slightly after injecting the water, while the permeability declines significantly after injecting the water. The degree of formation damage by the clay minerals decreases with increasing permeability. Formation damage is the most serious for cores with permeabilities smaller than $10 \times 10^{-3} \mu\text{m}^2$. In the different lithological cores, the grain size of argillaceous siltstone is the smallest, and the formation damage is the most serious after injecting the water. The average permeability is $7.47 \times 10^{-3} \mu\text{m}^2$ before injecting the water, and it decreases by 32.93% after injecting the water. The grain size of the siltstone is moderate, and the formation damage is moderate after injecting the water. The average permeability is $19.27 \times 10^{-3} \mu\text{m}^2$ before injecting the water, and it decreases by 23.37% after injecting the water. The grain size of the fine sandstone is the largest, and the formation damage is the lowest after injecting the water. The average permeability is $44.33 \times 10^{-3} \mu\text{m}^2$ before injecting the water, and it decreases by 17.45% after

Fig. 6 Kaolinite blockages in intergranular pores

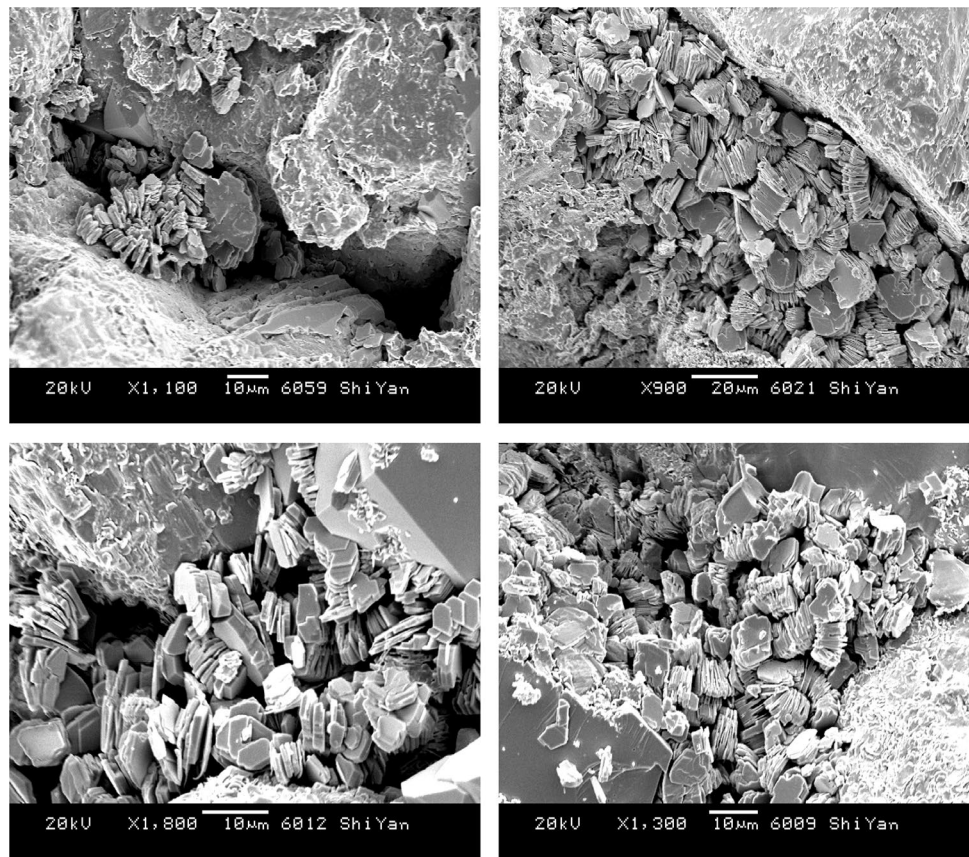
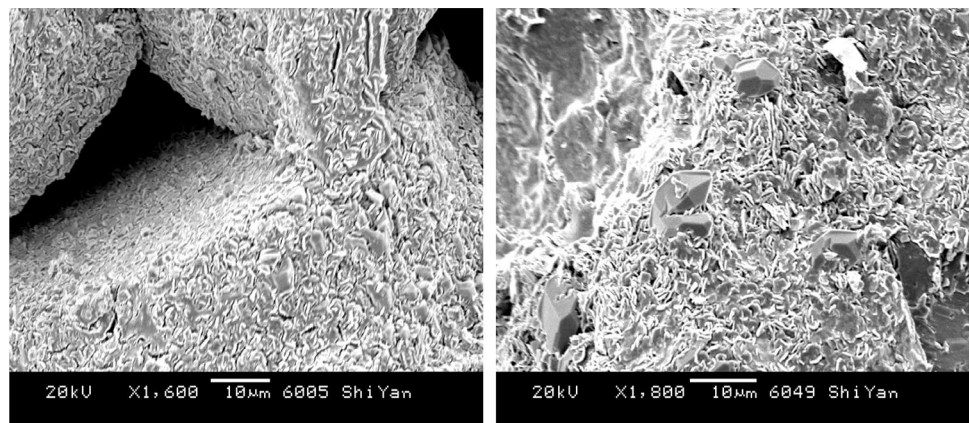


Fig. 7 Chlorite adhered onto particle surfaces before water injection



injecting the water. Therefore, water injection causes great damage to low permeability sandstone reservoirs of different lithologies. Before selecting and adjusting the injection scheme, it is necessary to conduct core damage experiments to evaluate the degree of damage in reservoirs caused by clay minerals.

Summary and conclusions

- (1) The low permeability sandstone reservoir in the Daqing oilfield contains 4 clay minerals: illite, kaolinites, chlorite and illite/smectite formations. The clay mineral

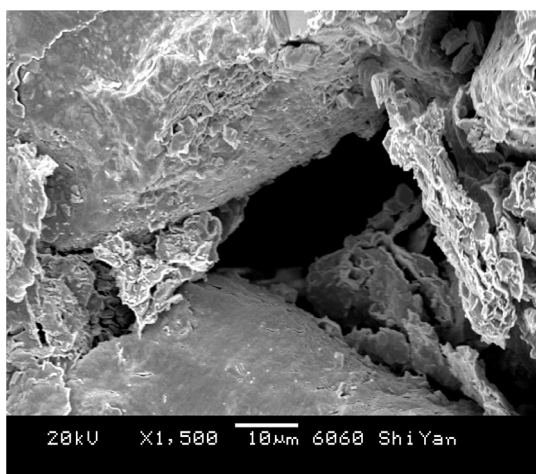


Fig. 8 Chlorite blockages in intergranular pores after water injection

content ranges from 6.78 to 14.14%. The clay mineral content decreases with increasing permeability.

- (2) After water injection, the content of clay minerals decreases by nearly 50%. The contents of illite, illite/smectite formation and chlorite decrease the most. Since the grain size of kaolinite is large, most kaolinite particles cannot pass through the pores and throats channels, and most cannot flow out of the cores with the fluid. The kaolinite content decreased by 32.75% after water injection. Kaolinites will migrate and block the pore-throats, which will lead to formation damage. Kaolinite blockages are more serious in argillaceous siltstones and siltstones than in sandstones.
- (3) After injecting the water, the porosity changes slightly, and the permeability is greatly reduced. With increasing permeability, the degree of formation damage by clay minerals decreases. After injecting the water, the

Table 4 Porosity and permeability before and after water injection

Core number	Lithology	Porosity (%)			Permeability ($10^{-3}\mu\text{m}^2$)		
		Before water injection	After water injection	Change rate (%)	Before water injection	After water injection	Reduction percentage (%)
#3	Argillaceous siltstone	20.7	20.6	-0.48	4.8	3.2	33.26
#14	Argillaceous siltstone	20.1	20.2	0.50	6.9	4.4	36.89
#19	Argillaceous siltstone	21.2	21.4	0.94	10.7	7.6	28.64
#20	Siltstone	22.1	21.9	-0.90	14.6	11.2	23.58
#23	Siltstone	21.2	21.3	0.47	18.7	14.1	24.65
#24	Siltstone	23.4	23.2	-0.85	24.5	19.1	21.87
#28	Fine sandstone	22.7	22.9	0.88	36.8	29.0	19.54
#30	Fine sandstone	22.8	22.9	0.44	42.1	34.2	18.68
#31	Fine sandstone	24.1	24.3	0.83	54.1	46.5	14.12

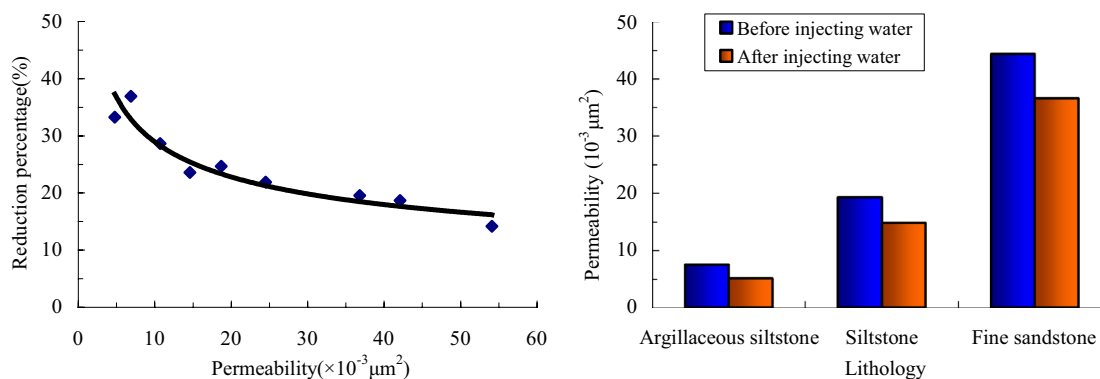


Fig. 9 Comparison of permeabilities in different lithological cores before and after water injection

Fig. 9 Comparison of permeabilities in different lithological cores before and after water injection

permeabilities of argillaceous siltstone, siltstone, and fine sandstone decrease by approximately 32.93, 23.37 and 17.45%, respectively.

Acknowledgements This work was supported by National Natural Science Foundation of China under Grant No. 12002083.

Funding No funding was secured for this manuscript.

Declarations

Conflict of interest The authors declare that they have no known competing financial interests or personal relationships that could have appeared to influence the work reported in this paper. On behalf of all the co-authors, the corresponding author states that there is no conflict of interest.

Open Access This article is licensed under a Creative Commons Attribution 4.0 International License, which permits use, sharing, adaptation, distribution and reproduction in any medium or format, as long as you give appropriate credit to the original author(s) and the source, provide a link to the Creative Commons licence, and indicate if changes were made. The images or other third party material in this article are included in the article's Creative Commons licence, unless indicated otherwise in a credit line to the material. If material is not included in the article's Creative Commons licence and your intended use is not permitted by statutory regulation or exceeds the permitted use, you will need to obtain permission directly from the copyright holder. To view a copy of this licence, visit <http://creativecommons.org/licenses/by/4.0/>.

References

- An SY, Yao J, Yang YF, Zhang L, Zhao JL, Gao Y (2016) Influence of pore structure parameters on flow characteristics based on a digital rock and the pore network model. *J Nat Gas Sci Eng* 31:156–163. <https://doi.org/10.1016/j.jngse.2016.03.009>
- Baker JC, Uwins PJR, Mackinnon ID (1993) ESEM study of authigenic chlorite acid sensitivity in sandstone reservoirs. *J Petrol Sci Eng* 8:269–277. [https://doi.org/10.1016/0920-4105\(93\)90004-X](https://doi.org/10.1016/0920-4105(93)90004-X)
- Cosenza P, Robinet JC, Prêt D, Huret E, Fleury M, Géraud Y et al (2014) Indirect estimation of the clay content of clay-rocks using acoustic measurements: New insights from the Montiers-sur-Saulx deep borehole (Meuse, France). *Mar Petrol Geol* 53:117–132. <https://doi.org/10.1016/j.marpetgeo.2013.07.004>
- Demirel IH (2005) Whole-Rock, clay mineral contents and matrix effect on the cenomanian/turonian petroleum source rocks in the Lower Antalya Nappe, Western Taurus Region of Turkey. *Petrol Sci Technol* 23:1183–1197. <https://doi.org/10.1081/LFT-200035556>
- Grude S, Dvorkin J, Landrø M (2015) Permeability variation with porosity, pore space geometry, and cement type: a case history from the Snøhvit field, the Barents Sea. *Geophysics* 80:D43–D49. <https://doi.org/10.1190/geo2014-0064.1>
- Jain AK, Ahmed K, Ferdous H, Mishra P, Al-Matrouk M, Al-Ali Y et al (2016) An experimental investigation of steam induced permeability changes in clay bearing formation of North Kuwait. *Proc-SPE EOR Conf*. <https://doi.org/10.2118/179762-MS>
- Jiang L, Sun J, Liu X (2012) Pore-space microstructure and clay content effect on the elastic properties of sandstones. *Petrol Sci Technol* 30:830–840. <https://doi.org/10.1080/10916466.2010.492372>
- Kamal MS, Mahmoud M, Hanfi M, Elkhatny S, Hussein I (2019) Clay minerals damage quantification in sandstone rocks using core flooding and NMR. *J Petrol Explor Prod Technol* 9:593–603. <https://doi.org/10.1007/s13202-018-0507-7>
- Law S, McDonald A, Fellows S, Reed J, Sutcliffe PG (2015) Influence of clay content and type on oil recovery under low salinity waterflooding in North Sea Reservoirs. *Proc-SPE Offshore Europe Conf Exhibition*. <https://doi.org/10.2118/175506-MS>
- Li DL, Zha WS, Liu SF, Wang L, Lu DT (2016) Pressure transient analysis of low permeability reservoir with pseudo threshold pressure gradient. *J Petrol Sci Eng* 147:308–316. <https://doi.org/10.1016/j.petrol.2016.05.036>
- Ma K, Jiang H, Li J, Zhao L (2016) Experimental study on the micro alkali sensitivity damage mechanism in low-permeability reservoirs using QEMSCAN. *Nat Gas Sci Eng* 36:1004–1017. <https://doi.org/10.1016/j.jngse.2016.06.056>
- Meng M, Ge HK, Ji WM, Wang XQ, Chen L (2015) Investigation on the variation of shale permeability with spontaneous imbibition time: Sandstones and volcanic rocks as comparative study. *J Nat Gas Sci Eng* 27:1546–1554. <https://doi.org/10.1016/j.jngse.2015.10.019>
- Olayiwola SO, Dejam M (2020) Synergistic interaction of nanoparticles with low salinity water and surfactant during alternating injection into sandstone reservoirs to improve oil recovery and reduce formation damage. *J Mol Liq* 317:114228. <https://doi.org/10.1016/j.molliq.2020.114228>
- Peng SM, Yin X, Zhang JC, Li JM, Ren JB, Wang FG (2006) Evolutionary pattern of clay mineral and rock sensitivity in water-flooding reservoir. *Acta Petrolei Sinica* 27:71–75. <https://doi.org/10.7623/syxb200604016>
- Reuvers N, Golombok M (2009) Shear rate and permeability in water flooding. *Transport Porous Med* 79: 249–253. <https://doi.org/10.1007/s11242-008-9313-x.pdf>
- Sadhukhan S, Dutta T, Tarafdar S (2007) Simulation of diagenesis and permeability variation in two-dimensional rock structure. *Geophys J Int* 169:1366–1375. <https://doi.org/10.1111/j.1365-246X.2007.03426.x>
- Sameni A, Pourafshary P, Ghanbarzadeh M, Ayatollahi S (2015) Effect of nanoparticles on clay swelling and migration. *Egypt J Pet* 24:429–437. <https://doi.org/10.1016/j.ejpe.2015.10.006>
- Strand S, Hjuler ML, Torsvik R, Pedersen JI, Madland MV, Austad T (2007) Wettability of chalk: impact of silica, clay content and mechanical properties. *Petrol Geosci* 13:69–80. <https://doi.org/10.1144/1354-079305-696>
- Stück H, Plagge R, Siegesmund S (2013) Numerical modeling of moisture transport in sandstone: the influence of pore space, fabric and clay content. *Environ Earth Sci* 69:1161–1187. <https://doi.org/10.1007/s12665-013-2405-0>
- Wang B, Qin Y, Shen J, Wang G, Zhang Q, Liu M (2019a) Experimental study on water sensitivity and salt sensitivity of lignite reservoir under different pH. *J Petrol Sci Eng* 172:1202–1214. <https://doi.org/10.1016/j.petrol.2018.09.036>
- Wang DQ, Yin DY, Gong XZ (2019b) Numerical simulation of microemulsion flooding in low-permeability reservoir. *J Chem* 2019:1–8. <https://doi.org/10.1155/2019/5021473>
- Wang DQ, Yin DY, Zhou YZ (2019c) Fine classification of ultra-low permeability reservoirs around the Placanticline of Daqing oilfield (PR of China). *J Petrol Sci Eng* 174:1042–1052. <https://doi.org/10.1016/j.petrol.2018.12.008>
- Wang L, Zhang H, Peng XD, Wang PR, Zhao N, Chu SS et al (2019d) Water-sensitive damage mechanism and the injection water source optimization of low permeability sandy conglomerate reservoirs. *Petrol Explor Dev* 46(6):1218–1230. [https://doi.org/10.1016/S1876-3804\(19\)60275-2](https://doi.org/10.1016/S1876-3804(19)60275-2)

- Yue WZ, Tao G, Chai XY, Jiang HX, Mu HW (2011) Investigation of effects of clay content on F- ϕ relationship by Lattice gas automation using digital rock model. *Petrol Sci* 8:170–176. <https://doi.org/10.1007/s12182-011-0131-3>
- Zhang CL, Wang P, Song GL, Qu GD, Liu JL (2017) Optimization and evaluation of binary composite foam system with low interfacial tension in low permeability fractured reservoir with high salinity. *J Petrol Sci Eng* 160:247–257. <https://doi.org/10.1016/j.petrol.2017.10.047>
- Zheng JW, Yu L, Sun DQ (2009) Main affecting factors and special technologies for exploration and exploitation of low-permeability oil and gas resources. *Natural Gas Geosci* 20:651–656. <https://doi.org/10.11764/j.issn.1672-1926.2009.05.651>
- Zhou YZ, Yin DY, Cao R, Zhang CL (2018) The mechanism for pore-throat scale emulsion displacing residual oil after water flooding. *J Petrol Sci Eng* 163:519–525. <https://doi.org/10.1016/j.petrol.2018.01.027>
- Zhou YZ, Yin DY, Chen WL, Liu B, Zhang XR (2019) A comprehensive review of emulsion and its field application for enhanced oil recovery. *Energy Sci Eng* 7:1046–1058. <https://doi.org/10.1002/ese3.354>

Publisher's Note Springer Nature remains neutral with regard to jurisdictional claims in published maps and institutional affiliations.